Action of Melittin on the DPPC-Cholesterol Liquid-Ordered Phase: A Solid State ^{2}H- and ^{31}P-NMR Study

Tanja Pott and Erick J. Dufourc
Centre de Recherche Paul Pascal, Centre National de la Recherche Scientifique, 3600 Pessac, France

ABSTRACT Solid-state deuterium and phosphorus-31 nuclear magnetic resonance studies of deuterium-labeled β-[2,2′,3,4,4′,6-$^2H_6$]-cholesterol and 1,2-dipalmitoyl-*sn*-glycero-3-phosphatidylcholine have been undertaken to monitor the action of melittin on model membranes containing 30 mol% cholesterol, both at the molecular and macroscopic level. Cholesterol totally inhibits the toxin-triggered formation of large unilamellar vesicles and strongly restricts the appearance of small discs. The latter remain stable over a wide temperature range (20–60°C) because of an increase in their cholesterol content as the temperature increases. This process is related to a constant disc hydrophobic thickness of ~29 Å. The system, when not in the form of discs, appears to be composed of very large vesicles on which melittin promotes magnetically induced ellipsoidal deformation. This deformation is the greatest when the maximum of discs is observed. A model to describe both the disc formation and stability is proposed.

INTRODUCTION

The amphiphilic polypeptide melittin consists of 26 amino acids and is the major compound of the european honey bee (*apis mellifera*) venom (~50% dry weight) (Habermann and Jentsch, 1967). One characteristic effect of melittin on cell membranes is its ability to lyse natural and artificial membranes (Sessa et al., 1969; Habermann, 1972). Melittin is amphiphilic with a net charge of +5 to +6 (for review, see Dempsey (1990) and references therein). Depending on concentration, ionic strength, and pH, it exists either as a monomer or tetramer in solution (Faucon et al., 1979). Although the monomer is mainly disordered, the tetramer and the membrane-associated species are highly α-helical (Drake and Hider, 1979; Lauterwein et al., 1979; Talbot et al., 1979; Terwilliger and Eisenberg, 1982). As far as the structure of membrane-associated melittin is concerned, different studies show a variability of results depending on the bilayer lipid composition, the lipid phase, and the hydration level (Brauner et al., 1987; Talbot et al., 1987; Vogel, 1987; Frey and Tamm, 1991; John and Jähnig, 1991; Maurer et al., 1991; Weaver et al., 1992). Of greater interest are the results obtained from fluid phase bilayers at high hydration level, which may be considered representative models for real membranes. Under these conditions, some studies propose that the axis of the helix lies parallel to the membrane surface (Brauner et al., 1987; Talbot et al., 1987), whereas others suggest that there are circumstances where transbilayer helical orientations are preferred (Vogel, 1987; John and Jähnig, 1991). In addition, its location with respect to the bilayer seems to change with temperature (Dufourc et al., 1986b; Talbot et al., 1987). On pure phosphatidylcholine (PC) membranes, melittin-induced membrane perturbations have been found to depend on the lipid physical state (gel or fluid phase). It has been shown that for lipid/peptide molar ratios, R_i, greater than 10 and up to 100, melittin disrupts gel phase PC membranes in small discoidal objects with diameter of 200–400 Å and a thickness comparable with that of a single bilayer (Dufourc et al., 1986a; Dufourcq et al., 1986). For $R_i > 100$ it is still unclear whether disk formation occurs. Interestingly, to exhibit such a behavior, the system must be incubated once above the gel-to-liquid crystalline transition temperature, T_C, of the pure lipid before cooling down in the gel phase (Dufourcq and Faucon, 1977; Dasseux et al., 1984; Dufourc et al., 1986a; Dempsey and Watts, 1987). A more recent study reports that an incubation above the pre transition temperature, T_{pre}, might be sufficient to obtain maximum melittin efficiency (Monette et al., 1993). Below T_{pre} the small PC/melittin discs are metastable, but a complete disappearance of discs is not observed before several hundred hours (Dufourc et al., 1986b). Above the gel-to-fluid phase transition of the pure lipid, melittin induces the formation of large unilamellar vesicles (LUV) with average diameter of about 4000 Å coexisting with some lipid multilayers (Dufourc et al., 1986a; Dufourcq et al., 1986). If the system has been incubated once, the disc-to-vesicle transition is reversible and directly related to the lipids state, i.e., it takes place at about T_C. For higher doses of melittin ($R_i <$ 10), the disc-to-vesicle transition no longer exists and the system is under the form of small objects (100–200 Å diameter), whatever the temperature.

Cholesterol is a major component of plasma membranes in many cells of higher organisms, making up as much as 45% (weight) of the lipid fraction in the case of the erythrocyte membrane, and is known to act as a regulator of membrane fluidity. The effects of elevated cholesterol concentrations (≥22%) on membranes in general may be summarized as follows. (i) The gel-to-fluid phase transition of model membranes is reduced or abolished. (ii) There is a decrease and increase in orientational order of the lipid

Received for publication 7 July 1994 and in final form 28 November 1994.
Address reprint requests to Dr. Erick J. Dufourc, Centre de Recherche Paul Pascal, CNRS, Av. A. Schweitzer, 33600 Pessac, France. Tel.: 33-568-45638; Fax: 33-568-45600; E-mail: dufourc@crpp.u-bordeaux.fr.

0006-3495/95/03/965/13 $2.00

chains in gel and fluid phases of model membranes, respectively. (iii) Fluid-like macroscopic properties are observed in a wide range of temperatures. (iv) The rotational diffusion of the lipid molecules is not greatly affected by the presence of cholesterol. (v) A reduction in permeability and a concomitant increase in membrane cohesion are detected (for an overview, see Yeagle (1985) and references therein). Its effect on phosphatidylcholine bilayers in excess water has been investigated by numerous studies and a variety of methods (Brown and Seelig, 1978; Marbrey et al., 1978; Needham et al., 1988; Sankaram and Thompson, 1990; Vist and Davis, 1990; McMullen et al., 1993). Its average orientation is quasi-perpendicular to the membrane surface, anchored with its polar hydroxyl group in the polar region of the bilayer and its hydrophobic body inside the core. This orientation has been reported to be temperature-independent over a temperature range from 10 to 65°C (Dufourc et al., 1984) and for concentrations varying from 10 to 50% in the bilayer (Léonard and Dufourc, 1991). Simulation of the phase behavior of the 1,2-dipalmitoyl-*sn*-glycero-3-phosphocholine (DPPC)/cholesterol system has been carried out (Ipsen et al., 1987; Ipsen et al., 1990; Scott, 1991) and is in accordance with the experimental phase diagram of Vist and Davis (1990) based on differential scanning calorimetry (DSC) and ^{2}H-NMR data. The most important feature of this two-component system is the elimination of the gel-to-fluid phase transition and the appearance of the β- or liquid-ordered phase at sterol concentrations higher than 22 mol%.

Because it is likely that this phase is of biological relevance, especially for modeling perturbations on outer plasma membrane, details about the action of melittin on the liquid-ordered phase should improve the understanding of biological membrane interactions with small peptides, as a model for membrane-protein interactions in general. In this context, it was the aim of our study to investigate the peptide/membrane interaction on the macroscopic as well as on the microscopic level.

Solid state deuterium and phosphorus-31 nuclear magnetic resonance (^{2}H- and ^{31}P-NMR) are proven to be powerful techniques to monitor polymorphic behavior (macroscopic), because different motional phases are characterized by different correlation times and, consequently, different spectral shapes. According to Seelig and Seelig (1980), an isotropic NMR line may correspond to different nonlamellar structures, such as vesicles, micelles, discs, etc., undergoing fast isotropic motions, whereas extended lamellar assemblies result in a powder pattern. Especially, ^{31}P-NMR lineshapes are very sensitive to the size of objects undergoing isotropic tumbling (Burnell et al., 1980). On a microscopic level, both NMR techniques reveal information about melittin-induced perturbations in extended bilayer assemblies at the polar headgroup level (^{31}P-NMR) and the hydrophobic core of the membrane (^{2}H-NMR). The combination of ^{31}P-NMR of the DPPC molecule and ^{2}H-NMR of β-[2,2′,3,4,4′,6-$^2H_6$]-cholesterol has the unique advantage that one can follow in situ the melittin-induced polymorphic behavior from both the phospholipid and cholesterol point of view.

MATERIALS AND METHODS

Synthetic DPPC and β-cholesterol were purchased from Sigma Chemical Co. (Ste Quentin-fallavier, France) and used without further purification. [2,2′,3,4,4′,6-$^2H_6$]-cholesterol was synthesized according to published procedures (Dufourc et al., 1984). Highly purified melittin was obtained from Fluka (Ste Quentin-fallavier, France) and also used without further purification. Thin layer chromatography has been performed before and after experiments. No lysophosphatidylcholine was detected in any sample after completion of NMR experiments.

Lipid dispersions were prepared according to established procedures (Dufourc et al., 1984). The dry lipid powder was dispersed in the appropriate buffer, then heated to 50–60°C, vortexed, and cooled down until freezing of the sample. This cycle was repeated at least 5 times until a homogeneous dispersion was obtained. In the case of cholesterol-containing systems, lipids and cholesterol first were dissolved in chloroform/methanol (2:1 v/v), mixed, and the solvent then was removed by blowing a stream of nitrogen over the sample. To ensure that all organic solvents were removed, the sample was pumped under vacuum overnight. Melittin was dissolved in the same buffer as was used for the lipids and added directly, followed by incubation at 50°C for at least 30 min and vigorous vortexing. A Tris buffer system (pH 7.5) containing 10 mM EDTA and 100 mM NaCl (such a NaCl concentration provides a tetrameric state of the toxin in solution (Faucon et al., 1979; Talbot et al., 1979; Bello et al., 1982; Podo et al., 1982)) was used. ^{31}P-NMR samples usually contained 50 mg of phospholipid in 1 ml of buffer and, in the case of ^{2}H-NMR on deuterated cholesterol, 200 mg of phospholipid in 1 ml of buffer.

^{31}P-NMR was carried out on a Bruker WH 270 implemented for high power solid state spectroscopy and operating at 109.35 MHz; phase cycled Hahn-echo pulse sequence (Rance and Byrd, 1983) and gated proton decoupling were used. ^{2}H-NMR experiments were performed on a Bruker MSL 200 operating at 30.7 MHz by means of a quadrupolar echo composite pulse sequence (Levitt and Freeman, 1981; Levitt, 1982). Quadrature detection was used in both cases. Samples were allowed to equilibrate at least 30 min at a given temperature before the NMR signal was acquired; the temperature was regulated to ±1°C. Typical acquisition parameters were: a spectral window of 50 kHz (^{31}P-NMR) or 500 kHz (^{2}H-NMR); 90° pulsewidth of 8 and 4 μs (^{31}P-NMR, ^{2}H-NMR of labeled cholesterol, respectively); delay τ between the two pulses of 40 μs in all cases; recycle delay for ^{31}P-NMR of 6–8 s and for ^{2}H-NMR of 80 ms; number of scans, 1,000–1,500 and 50,000 (^{31}P-NMR, ^{2}H-NMR, respectively). T_{2e} was measured according to Dufourc et al. (1992). Data treatment was accomplished on Aspect 2000, 3000, and Vax/VMS 8600 computers; spectral de-Paking and T_{2e} analyses were performed as described by Bloom et al. (1981), Sternin et al. (1983) and MacDonald (1980), respectively. The de-Paked spectra were calculated for bilayer normals oriented at 90° with respect to the magnetic field direction. The amount of isotropic line superimposed on a powder pattern was determined by simulation of a Gaussian or Lorentzian line and subsequent subtraction from the experimental spectrum (T. Pott and E. J. Dufourc, unpublished data). Percentages are expressed relative to the total spectral area.

RESULTS

Experiments were performed for phospholipid/peptide molar ratios, R_i, of ∞, 100, 50, 20, and 10; in the case of ^{2}H-NMR, an additional $R_i = 4$ was investigated. Thermal variations were always carried out by decreasing temperature.

Fig. 1 shows selected ^{31}P-NMR spectra for the thermal variation of the DPPC/melittin system at $R_i = 20$ in the absence (*left*) and the presence (*middle*) of 30 mol% cholesterol as well as the corresponding ^{2}H-NMR spectra of labeled cholesterol (*right*). ^{31}P-NMR spectra of the DPPC/melittin system above T_C show a broad and slightly asymmetric line (linewidth at half height, $\Delta\nu_{1/2}$ = 500–1500 Hz). In contrast, in the lipids gel phase, a narrow and symmetric line is de-

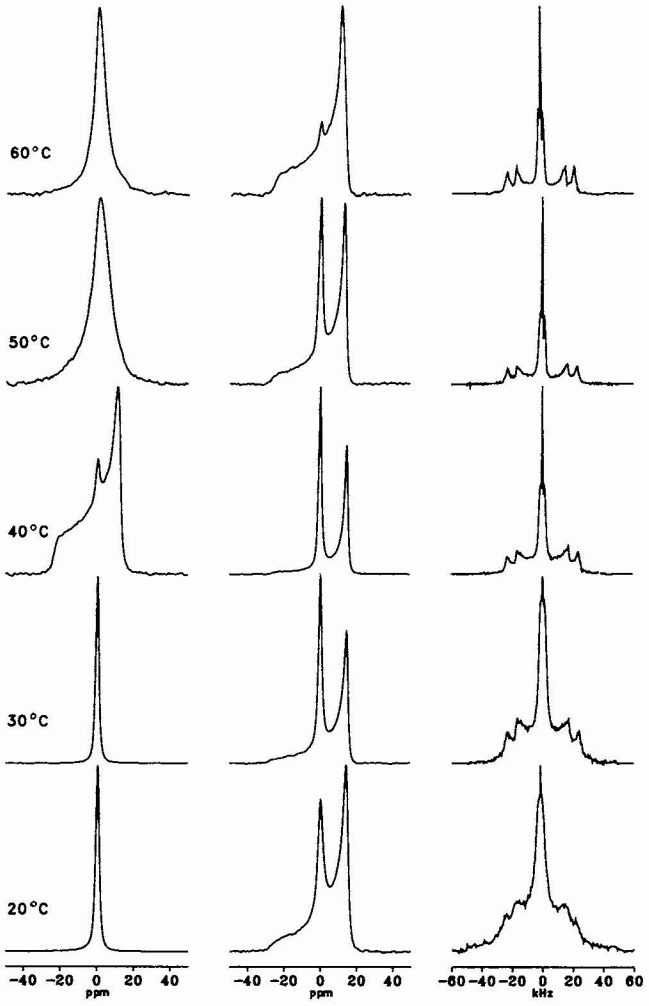

FIGURE 1 ^{31}P- and ^{2}H-NMR spectra of the melittin/DPPC system in the presence and absence of cholesterol. The left column shows ^{31}P-NMR spectra for selected temperatures of the cholesterol-free system at $R_i = 20$. The corresponding ^{31}P-NMR and ^{2}H-NMR spectra of the system containing 30 mol% cholesterol are presented in the middle and right columns, respectively.

tected ($\Delta\nu_{1/2}$ = 200–400 Hz). At 40°C, i.e. at about T_C, a typical powder pattern of an extended bilayer is obtained, superimposed only by a small fraction of isotropic line (≈6%). For the 30 mol% cholesterol-containing system and despite the quite important quantity of melittin added, the amount of isotropic line does not exceed 54%. This is the maximal value, obtained near T_C. The linewidth, $\Delta\nu_{1/2}$, of the isotropic line does not undergo strong modifications (200–450 Hz), whatever the experimental conditions. Its width is comparable with that observed for the DPPC/melittin system in the gel phase.

Similar to what was observed with ^{31}P-NMR, the ^{2}H-NMR spectra show the superimposition of an isotropic line on a multiple powder pattern (due to nonequivalent C—^{2}H bond labels, Taylor et al., 1981). The cholesterol bilayer spectrum persists in the entire measured temperature range, and the melittin-induced isotropic line keeps almost the same linewidth (550–650 Hz). Percentages of isotropic line were determined as described in Materials and Methods. In the case of the sterol-free system at R_i = 20, the isotropic line is at about 100%, exception made for $T \approx T_C$; for higher toxin concentrations (R_i = 10), no powder pattern was observed over the entire temperature range (see also Dufourc et al., 1986a; Pott and Dufourc, 1993). For the cholesterol-containing system, these amounts, determined from ^{31}P- and ^{2}H-spectra and called iso^{DPPC} and iso^{chol}, respectively, are presented in Fig. 2. Up to R_i = 20, the amount of nonlamellar structures, i.e., the isotropic line, exhibits a maximum not only detected from the phospholipid but also from the cholesterol molecule. It is worth mentioning that the term "nonlamellar" is used herein to qualify systems that are not under the form of stacked lamellae, although they may locally exhibit a bilayer structure. The maximum in iso^{DPPC} takes place at about T_C, with a slight shift to higher temperatures at R_i = 20. Furthermore, the increase in iso^{DPPC} with increasing temperature is apparently linear. With increasing melittin concentration, the fraction of nonlamellarly organized DPPC increases for all temperatures, exception made for 60°C. The amount of cholesterol in the nonlamellar environment, i.e., iso^{chol}, exhibits a similar evolution (up to R_i = 20), but the iso^{chol} maximum is displaced to somewhat higher temperatures (≈50°C). Despite these similarities, except for the high temperature region, the amounts of isotropic line obtained

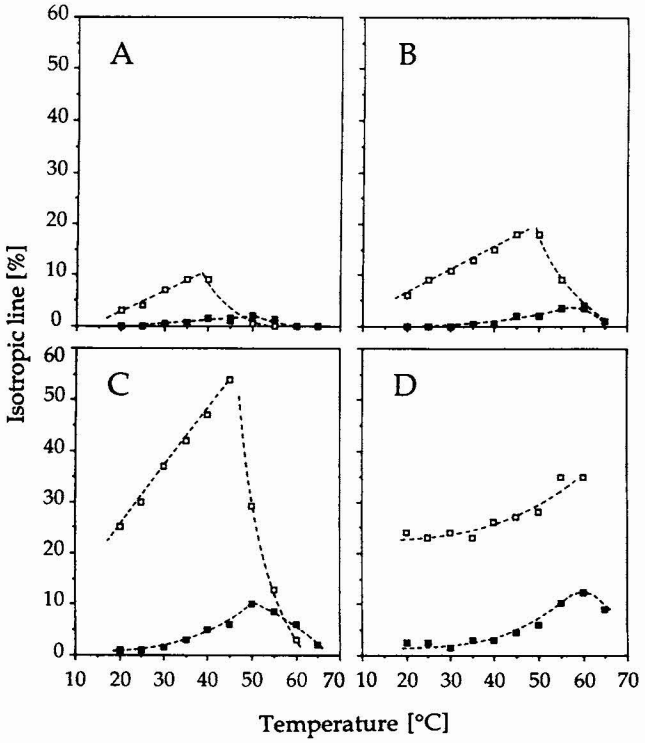

FIGURE 2 Percentages of isotropic line as a function of temperature for different phospholipid/melittin molar ratios. (*A*) R_i = 100; (*B*) R_i = 50; (*C*) R_i = 20; (*D*) R_i = 10. Percentages are expressed relative to the total spectral area. Filled symbols correspond to isotropic line% measured on ^{2}H-NMR spectra of ^{2}H-labeled cholesterol, open symbols to that measured on ^{31}P-NMR spectra. Accuracy in area determination is ±1%. Dashed lines are drawn to help read the figure.

from cholesterol are much less compared with those measured from the phospholipids. In contrast, at high temperatures this overweight of ^{31}P-NMR isotropic line is no longer detected, and the percentages of nonlamellar structures are close for both kinds of lipid.

Surprisingly, at $R_i = 10$ and in the temperature range from 25 to 45°C, markedly lower amounts of nonlamellarly arranged DPPC (with respect to $R_i = 20$) are found, although the system contains the double quantity of toxin. From 20 to 60°C no maximum is observed, but a continuous nonlinear increase with increasing temperature is observed. The thermal evolution of cholesterol in nonlamellar structures parallels that of the lipid with, however, lower amounts of isotropic line, i.e., $iso^{chol} \approx iso^{DPPC} - 22\%$. Spectra of the sample with labeled cholesterol were also obtained at 65°C; the drop down of iso^{chol} at this temperature may indicate the existence of a maximum of nonlamellar lipids shifted to ≈60°C. From Fig. 2 it is obvious that the system containing very high amounts of melittin, i.e., $R_i = 10$, behaves quite differently compared with those of $R_i = 100$, 50, and 20.

As far as the headgroup region is concerned, the presence of low amounts of melittin barely affects the chemical shift anisotropy, $\Delta\sigma$, of the remaining powder pattern (data not shown). The only exception is observed for the $R_i = 20$ system at $T \geq 50$°C, where a ~10% decrease of $\Delta\sigma$ occurs with increasing temperature. Interestingly, $\Delta\sigma$ passes through a weak maximum between 30 and 40°C that becomes more pronounced with increasing peptide concentration, except for $R_i = 10$, where the weak maximum is comparable with the toxin-free system. Furthermore, one notes an overrepresentation of the 90° orientation for ^{31}P-NMR spectra, which exhibit important quantities of isotropic lines (Fig. 1, *middle*).

The anisotropic β-[2,2′,3,4,4′,6-$^2H_6$]-cholesterol ^{2}H-NMR spectrum consists of three superimposed powder patterns corresponding to different deuterium-labeled positions in the structure; the assignment for the quadrupolar splittings is $\Delta\nu_Q$(C-2, 4 axial) > $\Delta\nu_Q$(C-2, 4 equatorial) > $\Delta\nu_Q$(C-6) (Taylor et al., 1981; Dufourc et al., 1984). Differences between the 2 and 4 equatorial positions, due to the slightly different orientation of these bonds with respect to the main axis of motion of the fused ring system, are not resolved (see also inset in Fig. 3). Also, the label at position 3 is not resolved and has a quadrupolar splitting near those of the 2 and 4 axial positions (Taylor et al., 1981; Dufourc et al., 1984).

To check whether melittin alters the orientation of cholesterol in the membrane, anisotropic ^{2}H-NMR spectra of the labeled sterol were thereupon analyzed by testing whether the ratio of quadrupolar splittings, $\Delta\nu_Q$, originating from different C—^{2}H bonds on the fused ring system stays approximately constant (Dufourc et al., 1984; Léonard and Dufourc, 1991). $\Delta\nu_Q$(C-2,4 ax) and $\Delta\nu_Q$(C-2,4 eq) were used, and their ratio was found to stay invariant, within acceptable deviations, for all temperatures and melittin concentrations used herein. This indicates that cholesterol orientation stays unchanged and perpendicular to the bilayer surface. However, the principal source of error in this kind of treatment lies in

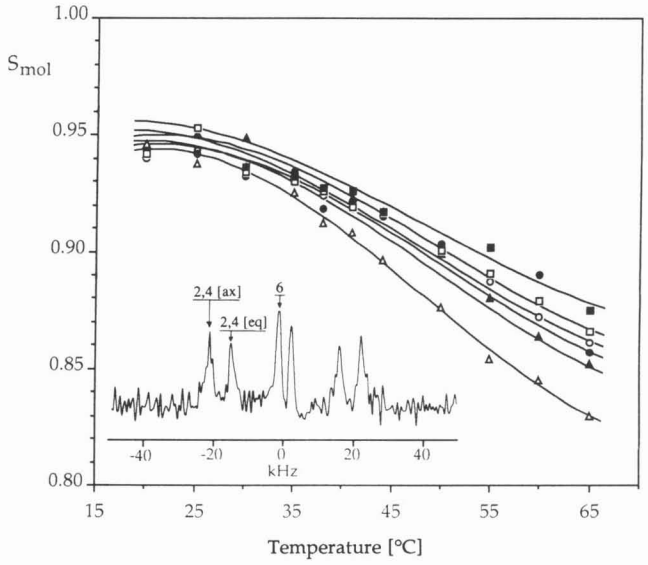

FIGURE 3 Molecular order parameter of cholesterol versus temperature for various R_i. △, $R_i = \infty$; ▲, $R_i = 100$; ○, $R_i = 50$; ●, $R_i = 20$; □, $R_i = 10$; ■, $R_i = 4$. In the inset, a de-Paked spectrum of the labeled cholesterol in the melittin-DPPC-cholesterol system is shown. Assignment of ^{2}H-labeled positions is described in the text. Solid lines result from polynomial fit of the data and are shown to improve readability of the figure.

the determination of the $\Delta\nu_Q$ values, taken from the de-Paked spectra (see *inset*, Fig. 3) and will not reveal small modifications of the average sterol orientation in the bilayer upon melittin addition.

As a consequence of the invariance of the cholesterol orientation, the molecular order parameter, S_{mol}, can be determined according to

$$S_{mol} = \Delta\nu_Q \left\{ \frac{3}{4} A_Q \frac{(3\cos^2\gamma - 1)}{2} \right\}^{-1}$$

(Taylor et al., 1981; Dufourc et al., 1984). $A_Q = 168$ kHz is the quadrupolar coupling constant for C—^{2}H bonds (Burnett and Müller, 1978), and γ is the angle between the sterol main axis of motion and the C—^{2}H bond axis. γ values were taken from Taylor et al. (1981) and are 68°, 75°, and 77° for C-2,4eq, C-2ax, and C-4ax, respectively. Because the axial positions are not resolved in our spectra, a $\gamma = 76°$ value was used for both. Resulting S_{mol} values are plotted in Fig. 3 as a function of temperature and melittin content.

For temperatures below 45°C and as a consequence of the quite scattered values in this temperature range, no modification of S_{mol} upon melittin addition is observed. In the range of 45–50°C, the molecular order parameter of the sterol is slightly, but significantly, higher in the presence of the peptide than in its absence, but is not affected further by an increase in melittin concentration. For the highest measured temperatures (60 and 65°C) and highest melittin content, S_{mol} appears to increase by no more than 5%, which is fully consistent with what is reported by Monette et al. (1993) for the influence of melittin ($R_i = 25$) on DPPC-$^2H_{62}$ model membranes containing 30 mol% cholesterol. These findings, however, are highly contrasting with the effect of melittin on the

DPPC/melittin system in the absence of cholesterol, where at high temperature (65°C, R_i = 20), melittin induces a decrease of S_{C-^2H} (Dufourc et al., 1986b).

Because we have determined the amounts of nonlamellar (discs) and lamellar phases using both DPPC and labeled cholesterol (Fig. 2), it is possible to calculate the amount of cholesterol in both phases. The evolution with temperature of the cholesterol concentration in the discs is reflected unambiguously in Fig. 4. For melittin concentrations up to R_i = 20, the cholesterol amount in the lamellar phase increases quasi-linearly with increasing temperature, passes through a maximum, and decreases with a further increase in temperature. In contrast, the evolution of the cholesterol content in the discs increases continuously with increasing temperature, whatever the R_i values. The increase of cholesterol concentration both in the lamellar phase and in the discs between 20 and 40°C may appear contradictory but is easily understood by considering that the amount of each phase varies with temperature (Fig. 2). For instance, at R_i = 20 and 20°C, 1 and 25% isotropic line are observed for cholesterol and phospholipid, respectively. Because the global amount of cholesterol versus lipid (phospholipid + cholesterol) is 30%, one determines the total lipid amount under the form of discs, the percentage of sterol in the discoidal and lamellar phase, and finds 17.8, 1.7, and 36.1%, respectively. At 40°C cholesterol and phospholipid give rise to 5 and 47% isotropic line, respectively, which leads to 34.4% of the total lipid organized as discs and to a cholesterol concentration in discs and lamellar phase of 4.4 and 43.5%. It is further noteworthy that the sterol concentration in the discs is always lower than the initial 30 mol%, exception made for 60°C.

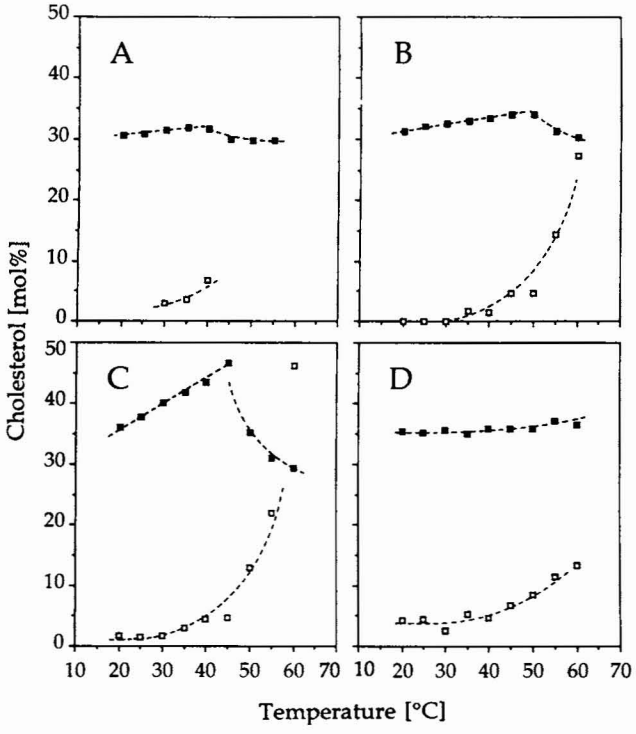

FIGURE 4 Calculated amounts of cholesterol versus temperature in the lamellar phase (*filled symbols*) and in the discs (*open symbols*) for different melittin contents. (*A*) R_i = 100; (*B*) R_i = 50; (*C*) R_i = 20; (*D*) R_i = 10. Accuracy for the cholesterol concentration in the lamellar phase is ±1% units; up to 15 mol% cholesterol contents in the discs, it is estimated to be ±2% units; for higher concentrations, ±7% units. Dashed lines are drawn to help read the figure.

Up to ≈40°C (T_C of the pure DPPC system and phase boundary for DPPC/melittin discs), the small objects contain very low amounts of cholesterol (≤7 mol%). It is then straightforward to conclude that the small objects formed for $T < T_C$, from the system initially containing 30 mol% cholesterol, are discs probably very similar to those of the pure DPPC/melittin system. It is further known that melittin can only promote the formation of the discs for gel-phase PCs, i.e., with a "rigid" membrane (Dufourc et al., 1986a). It appears, therefore, that the stability of such melittin-induced discs requires a certain rigidity of the bilayer. On the other hand, it is well established that cholesterol, for $T > T_C$, strongly inhibits *cis-trans* isomerization of the lipid fatty acyl chains, thus making the membrane more rigid (condensing effect of cholesterol). The increase in sterol content in the small objects with increasing temperature ($T > T_C$) is therefore necessary for disc stabilization.

Concentrations of sterol in discs and extended bilayers were also reported by Monette et al. (1993). Contrary to our in situ approach, they were estimated by chemical analysis after separation of both phases to be 9–23 mol% in the small objects and 36–39 mol% in the lamellar phase. Albeit these percentages can also be found in our study, some points have to be mentioned. First, it is not clear whether the physical separation of both phases interferes with an equilibrium between discs and lamellar phase. Second, although the authors report a temperature independence of the disc composition, their study was not done explicitly as a function of temperature.

DISCUSSION

Influence of cholesterol on the melittin-induced membrane fragmentation

The complete restructuration of the DPPC/melittin membrane is nicely visualized in Fig. 1 (*left* column), as is its disc-to-vesicle transition at about T_C, where a classical powder pattern is obtained. The observation of a powder pattern for the 30 mol% cholesterol-containing system whatever the temperature or melittin concentration shows clearly that the melittin-induced membrane disruption is strongly restricted (Fig. 1, *middle* and *right*). This already has been reported elsewhere (Monette et al., 1993; Pott and Dufourc, 1993). A small object-to-large bilayer transition similar to that occurring on the sterol-free system was not detected, which is in accordance with what has been reported recently by Monette et al. (1993). However, in contrast to the pronounced maximum of membranes fragmentation in our study (up to R_i = 20, ^{31}P-NMR), these authors do not report a strong temperature dependence of this system. The average diameter of the DPPC/melittin LUVs has been determined by quasi-elastic light scattering, electron microscopy, and gel

filtration and range between 2000 and 4000 Å (Dufourc et al., 1986a, b; Dufourcq, 1986). The wide and slightly asymmetric ^{31}P-NMR lines observed for this system match very well with the theoretical predicted ones of such objects (Burnell et al., 1980; Douliez et al., 1994). Under conditions where such a LUV formation is expected, Monette et al. obtained typical extended bilayer spectra, which are often accompanied by an overrepresentation of intensity at the 90° position (Dempsey and Watts, 1987; Dempsey and Sternberg, 1991; Monette et al., 1993). Two explanations are possible for this apparent disagreement between their study and our's: (i) the viscosity of the medium might differ largely from study to study, and (ii) systems may orient macroscopically in the magnetic field. The first one is linked to slow vesicle tumbling and would not lead to a broad "isotropic line" with NMR. More likely is the second explanation; because of the accentuated 90° orientation, the bilayers are assumed to orient partially in the presence of a magnetic field. A model proposed by Dempsey and Watts (1987) and Dempsey and Sternberg (1991) suggests that the fusion event of the small discoidal objects in the presence of a strong magnetic field, occurring at about T_C, will lead to extended, flat bilayers oriented with the membrane plane parallel to the magnetic field. Obviously, such a behavior will be favored by NMR thermal variations with increasing temperature (Monette et al., 1993) but not with decreasing temperature as used in this study. We would like to emphasize that the formation of such magnetically induced flat structures is not comparable with the "natural" action of melittin (as detected by many other techniques) on PC model membranes for $T > T_C$ and cannot give any indication about the extent of melittin-induced LUV formation, in contrast to our work. At this point, we have to mention that we have acquired all ^{31}P-NMR spectra for both systems under exactly the same conditions (same buffer, incubation time, dilution, and acquisition with decreasing temperature). Therefore, comparison of the ^{31}P-NMR isotropic linewidths above T_C in the presence of the sterol with those obtained in its absence shows unambiguously that the peptide-promoted LUV formation is inhibited completely by 30 mol% cholesterol.

The total inhibition of the LUV formation can be understood by a quite simple approach. To induce LUV formation, the peptide is expected to be localized in the headgroup region (see also Dufourc et al., 1986b), acting like a spacer of the choline groups, thus promoting positive bilayer curvature (Batenburg and De Kruijff, 1988). The sterol, located in the bilayer hydrophobic core, tightens the contact between the fatty acyl chains and, thus, may counterbalance the induced curvature, thus inhibiting the MLV-to-LUV transformation.

Because the isotropic linewidths of the DPPC/cholesterol/melittin system are about the same as for the sterol-free system for $T < T_C$, one may suggest that in the presence of cholesterol the isotropic line also corresponds to small discoidal objects of about the same size as the discs, observed for the pure PC/melittin system in the gel phase (Dufourc et al., 1986a). Hence, the formation of these discs is strongly, but not completely, inhibited by the sterol. On the other hand, the discs are stabilized over a large temperature range (20–60°C) by the presence of cholesterol. Some evidence for disc formation in the cholesterol-containing system also arises from the study of Monette et al. (1993), where the melittin concentration has been kept constant ($R_i = 20$) and the amount of cholesterol varied. According to these authors, disc fusion was detected for cholesterol concentrations up to 20 mol%. The fusion appears to be shifted to higher temperatures as the amount of membrane-incorporated cholesterol increases. With further increase of sterol content to 30 mol%, as in our study, such a transition was no longer observed. This suggests a cholesterol-triggered, progressive stabilization of the discs at higher temperatures. It is noteworthy that the word "discs" will be used in the following in a hypothetical way, because the existence of discs in the cholesterol-containing system is not directly proved. Nonetheless, more evidence for their existence will be given in the course of this discussion.

For extremely high amounts of melittin (e.g., $R_i = 5$), modification in the peptide action already has been reported for the cholesterol-free system (Dufourc et al., 1986a, b; Dufourcq, 1986), i.e., neither discs nor LUVs are detected whatever the temperature, but small "lipidic particles" with diameter of about 120 Å are detected. ^{2}H-NMR spectra of cholesterol at comparable high melittin amounts ($R_i = 4$) exhibit almost no difference with respect to $R_i = 10$, indicating a saturation effect. This is in accordance with Monette et al. (1993), who reported by ^{31}P-NMR a saturation effect for the same system between $R_i = 20$ and $R_i = 5$.

Bilayer thickness of the discs

Fig. 4 shows that the sterol content in discs increases with temperature. Assuming that their shape and their melittin/lipid ratio stay about constant with temperature, the curve describing cholesterol variation versus temperature should be the same, independent of the toxin amount in the sample (up to $R_i = 20$) and could be related to a structural or dynamical property of the system, i.e., a suited degree of order in the membrane.

It is important to test whether this hypothesis is a requirement for disc formation and stabilization. The underlying ideas are here twofold: (i) discs are formed from a membrane with a well defined (well suited) order, and (ii) discs are stable when changing the temperature if there is a means to maintain this ordering value.

Quadrupolar splittings of chain-perdeuterated DPPC are a way to measure membrane ordering. Here the first spectral moment, M_1, was used to probe the overall chain ordering. M_1 is related to the average chain order parameter, $\langle |S_{C-^2H}| \rangle$, by Bloom et al. (1978) and Davis (1979): $\langle |S_{C-^2H}| \rangle = \sqrt{3}M_1/\pi A_Q$. Therefore, we have taken M_1 values from the well studied DPPC/cholesterol system (Fig. 8 in Vist and Davis, 1990). By choosing $M_1 \approx 6.4 \cdot 10^4$ rad/s, i.e., $\langle |S_{C-^2H}| \rangle \approx 0.21$, and taking the corresponding cholesterol concentrations and temperatures, one can plot the variation of cholesterol content in DPPC/cholesterol model

membranes versus temperature for that given degree of chain ordering (Fig. 5, *filled symbols*). As expected, cholesterol content in the bilayer has to increase to maintain a constant degree of order when the temperature increases. This graph has been superimposed by the cholesterol content of discs versus temperature of our study (Fig. 5, *open symbols*). It is important to mention that here the data of all systems with $R_i \geq 20$ were plotted together. The agreement between the two curves is very good and strongly supports the idea of a well defined lipid order value in the melittin/lipid discs and that, as a consequence, their sterol content has to increase for $T > T_C$ to keep this value constant. This ordering value corresponds to the transition region of the pure DPPC membrane, i.e. lower than for gel phase order, but higher than for L_α order. Interestingly, $M_1 \approx 6.4 \cdot 10^4$ rad/s is about the value detected for the DPPC-$^2H_{31}$/melittin system at $R_i = 20$ in the disc-to-vesicle transition region, when the discs formation just starts (thermal variation by decreasing temperature; Dufourc et al., 1986b). This further supports the need of a well suited order to form and stabilize the discs.

The existence of such a constant as described above implies further that a certain bilayer thickness is needed for disc formation. This is easily understandable on the basis of a disc-adapted modification of the mattress model developed by Mouritsen and Bloom (1984). When picturing the discs as a small circular piece of bilayer, where the open hydrophobic edges are covered by the peptide, one may imagine that the peptide hydrophobic surface has to match with these edges to allow disc formation. In fact, this kind of model, called "bicycle tire," was introduced already by Segrest (1977) in the case of apolipoproteins and was proposed to apply to melittin by Dufourcq et al. (1986). This is supported further by the capability of melittin to form such discs depending on the PC fatty acyl chain length. DPPC (C16) membranes are transformed easily by melittin to metastable discoidal objects ($T < T_C$) and stay stable for about 100 h, whereas DSPC (C18) remains only stable for about 50 h. In contrast to C16 and C18 systems, disc formation with DAPC (C20) multilayers does not occur when the temperature is slowly decreased. The system must be quenched into the gel phase to obtain small melittin/lipid complexes. Furthermore, these DAPC discs reorganize rapidly into extended bilayers, i.e., already after 6 h, 50% of the discs have returned to extended bilayers (Dufourc et al., 1989). The size of the discs when formed is quasi-invariant of lipid chain length. Thus, simple geometrical constraints might be responsible for the formation and stability of the melittin surrounded discs. One may express the $\langle | S_{C-^2H} | \rangle$ (or M_1) invariance described in the above paragraph in terms of the hydrophobic bilayer thickness, d_h, by Seelig and Seelig (1974), Schindler and Seelig (1975): $d_h = d_0(\langle | S_{C-^2H} | \rangle + 0.5)$. With $d_0 = 39.4$ Å for DPPC (Marcelja, 1974), one finds 28.7 Å for the discs (even for possible tilted, gel-like lipids, this length should be relevant to the associated peptide). This leads, with a somewhat reasonable value of 5.2 Å for the headgroup region (Marsh, 1990), to a total disc thickness of ≈39 Å. Because order profiles of PC lipids of different chain length are quasi-identical for reduced temperatures, $T - T_C$ (Morrow and Lu, 1991), one may estimate the hydrophobic bilayer thickness of DSPC and DAPC in the transition region. Taking $M_1 = 6.4 \cdot 10^4$ rad/s as in the above, leads to $d_h \approx 32.2$ and 35.8 Å for DSPC ($d_0 = 44.4$ Å) and DAPC ($d_0 = 49.4$ Å), respectively. Thus, it is understandable that when slowly passing through the transition region, DAPC is simply too long (total bilayer thickness of ≈46 Å) to be transformed into discs by the peptide. In contrast, taking a somewhat typical fluid phase M_1 value of $4.5 \cdot 10^4$ rad/s results in the case of DAPC in $d_h \approx 32.8$ Å, which appears to be an acceptable length to form discs by means of a rapid quench.

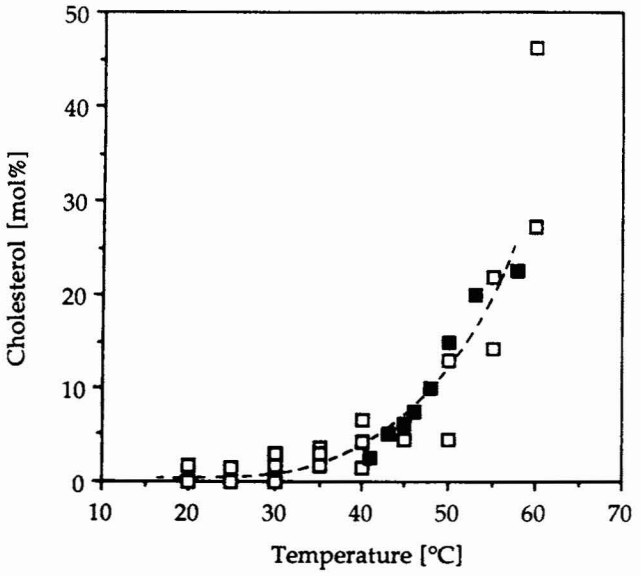

FIGURE 5 Correlation between cholesterol content in discs (melittin/DPPC/cholesterol) and in DPPC/cholesterol dispersions for a constant ordering. Open symbols represent the cholesterol concentration in the discoidal objects for $R_i = 100$, 50, and 20 as a function of temperature (Fig. 4). The filled symbols correspond to the cholesterol concentration of DPPC-$^2H_{62}$/cholesterol multilayers for a fixed value of $M_1 = 6.4 \times 10^4$ radians/s of the ^{2}H-NMR spectra. Values are taken from Fig. 8 in Vist and Davis (1990), and the corresponding temperatures were corrected by +3°C to account for the downshift in temperature induced by perdeuteration of DPPC acyl chains.

Based on this data, we will discuss briefly two possible orientations of melittin with respect to the disc plane: (i) the peptide surrounds the discs with the helical axis perpendicular to the disc plane or (ii) is parallel to it (see also Fig. 6). Assuming a 65% α-helical conformation of melittin as in solution (Dawson et al., 1978; Talbot et al., 1979; Bello et al., 1982), the α-helix 1–20 would be ≈30 Å long. This fits well the above estimated hydrophobic thickness, the charged COOH terminus then being arranged at the polar region. Picturing the peptide as a 100% α-helical rod results in a total helix length of ≈39 Å, which fits exactly the estimated total disc thickness for DPPC complexes. Such an orientation was also proposed by earlier studies (Dufourcq et al, 1986). On the other hand, the helices are ~10 ± 1 Å in diameter and by assuming a close contact between them this would result

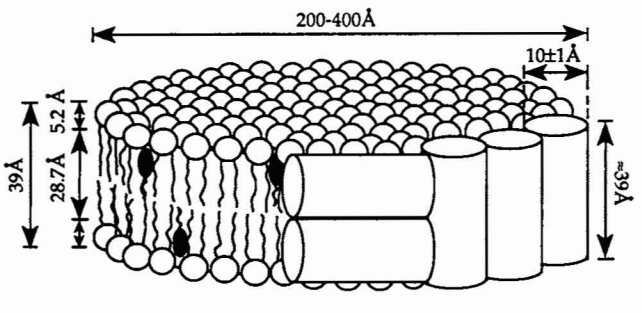

FIGURE 6 Schematic representation of the discs. Phospholipids and cholesterol are surrounded by melittin either with its helical axis parallel or perpendicular to the bilayer plane. Adapted from Dufourcq et al. (1986).

in ≈9 Å uncovered hydrophobic edge region for an arrangement of melittin parallel to the disc surface. Nevertheless, in the above, melittin is depicted as a perfect helical rod that clearly does not reflect its tridimensional structure. As a consequence, one may as well assume an inter-helical distance, which would also fit well a parallel orientation. To summarize, our data appear to be in favor of a quasi-transbilayer arrangement of the peptide at the disc edges, although case (ii) cannot be completely discarded.

Temperature dependence of the melittin-induced morphological changes

It has been pointed out earlier that the melittin-induced fragmentation for the cholesterol-free system is associated with the gel-to-fluid transition region of the lipid (Dasseux et al., 1984), where the coexistence of gel and fluid phase domains leads to several structural defects. The correlation of melittin-triggered membrane disruption with the pretransition (Monette et al., 1993) is not surprising, because the formation of "ripples" at the surface in the $P_{\beta'}$ phase is expected to cause structural defects. According to our study, fragmentation of the DPPC/melittin occurs at about T_{pre} but is not as efficient as after incubation at high temperature (data not shown). For the sterol-containing system, membrane disruption was found to be strongly suppressed if incubation was not performed. It seems likely that primary insertion (or association) of the peptide into the bilayer is favored by high temperatures, because the polar headgroup becomes more mobile, "diluted" with increasing thermal fluctuations of the fatty acyl chains and/or the molecule as a whole. We will distinguish, therefore, between peptide insertion and peptide-triggered mechanical breakdown of the membrane. Both phenomena might not necessarily occur at the same temperature.

The observed maximum of fragmentation for the 30 mol% cholesterol-containing system appears to be in disagreement with the usual picture of the β- or liquid-ordered phase, i.e., with a homogeneous phase over the relevant temperature range. One instead may invoke the theoretical cluster model, i.e., a heterogeneous membrane structure, for DPPC/cholesterol model membranes of (Cruzeiro-Hansson et al., 1989). Cluster formation means that below T_C domains of fluid phase are formed in the equilibrium gel phase, whereas above T_C domains of gel phase are formed in the equilibrium fluid phase. Increasing the amount of cholesterol leads according by this theoretical approach to a decrease in the average cluster size at about T_C, accompanied by an enhancement of cluster formation in the wings of the transition. For the 30 mol% cholesterol-containing DPPC bilayers, they must be in fast exchange because they have not yet been directly observed (NMR, Vist and Davis, 1990; ESR, Sankaram and Thompson, 1990; fluorescence, Parasassi et al., 1994).

Assuming that the melittin-induced membrane disruption is promoted by the occurrence of such defect lines, one may suggest that peptide efficiency on cholesterol-containing membranes is proportional to the cluster occurrence. Figuratively speaking, a melittin enrichment in these interfacial regions would result in a liberation of a disc, if the cluster has the appropriate cholesterol concentration (or the appropriate bilayer thickness) to be stable at a given temperature. An enhancement in cluster formation phenomena thus will result in an increase of probability for melittin to "find" a well constituted cluster.

Such a model might as well describe the sterol-free membrane. When lowering the temperature, the LUVs formed by the peptide stay stable until reaching the proximity of the transition. As mentioned above, important cluster formation occurs for the sterol-free system in a rather small temperature region. These clusters are thought to be of greater size than in presence of the sterol. The strong fluctuations of the membrane in the transition region thus will lead to a destruction of the LUVs resulting in their fusion to extended bilayer regions (see Fig. 1, 40°C), because the clusters might be of larger size than the discs. These extended bilayer regions, which give rise to the observed powder pattern, should be pictured as highly dynamic. On the other hand, these defect structures would allow the peptide to sink deeper into the bilayer core and finally to produce the discs. It might be worthwhile to point out again that the disc-to-vesicle transition is not a direct transition but occurs via an intermediate extended bilayer state.

Melittin-triggered orientation of a model membrane in a magnetic field

It has been mentioned already that under the influence of melittin (especially at $R_i = 20$) an accentuated 90° orientation was detected for the ^{31}P-NMR spectra. This can be seen more easily in Fig. 7, where such spectra ($R_i = 20$) are shown after elimination of the isotropic line. Three explanations might be possible. (i) Because the spectra were acquired by the use of the Hahn-echo pulse sequence, such an effect might be due to an angular dependence of T_{2e}. (ii) The membrane may partially orient in lamellar sheets, triggered by a fusion process, in coexistence with MLV. (iii) We may assume a magnetically induced ellipsoidal deformation of a

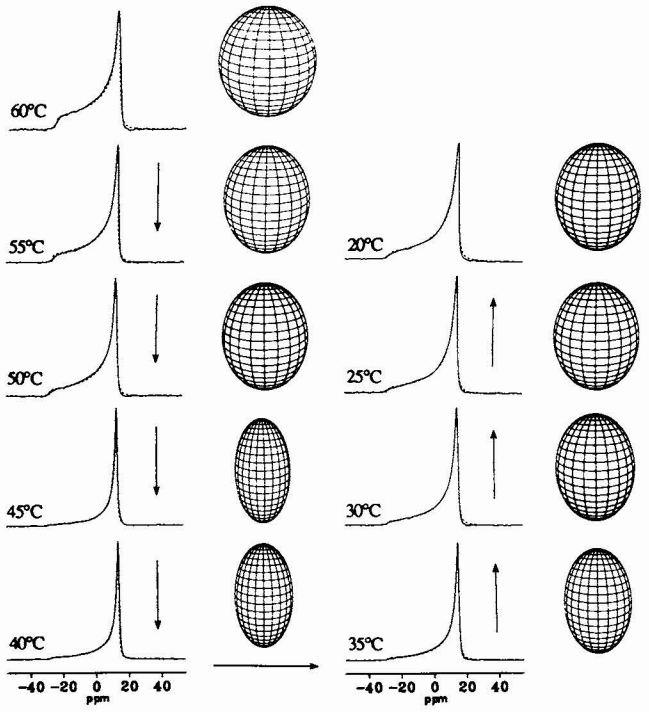

FIGURE 7 Full thermal variation of the DPPC/cholesterol/melittin system, $R_i = 20$, after elimination of the isotropic line from the experimental spectra. The dashed lines correspond to spectral simulations assuming an ellipsoidal deformation of the lipidic vesicles; the corresponding prolate is shown at the right-hand side of spectra. Arrows indicate the direction of the thermal variation. The long/short axis ratios in the prolates are as follows (decreasing temperature): 1.1; 1.3; 1.3; 2.0; 1.8; 1.6; 1.4; 1.3; 1.3.

formerly spherical vesicle, which will account for all of the anisotropic NMR signal.

As far as (i) is concerned, T_{2e} experiments were undertaken for the DPPC/cholesterol membrane in absence and presence ($R_i = 20$) of the peptide (data not shown). A temperature (40°C) was chosen where the most pronounced "orientational" effect was obtained (Fig. 7). Both systems show a slight increase of T_{2e} for 90° with respect to the 0° orientation, which should result in a small loss of intensity for the shoulder of the powder patterns when using the Hahn-echo sequence to record spectra. For the melittin-containing system, T_{2e} at 90° is somewhat more elevated. However, the angular variations of T_{2e} are not important enough to account for the observed effect. Thus, the powder patterns of spectra with such a 90° accentuation must correspond to magnetically induced orientation, (ii) or (iii), of the bilayer.

A coexistence of oriented sheets with MLV (ii) will lead for this anisotropic part of the system to a superposition of a powder pattern with an "isotropic" line centered at the 90° position. Simulations of the partially oriented experimental spectra by a combination of these two compounds were attempted but resulted in a clear disagreement between calculated and experimental spectra. Vesicle deformation of the DPPC/cholesterol system (30 mol%) into a prolate, giving rise to such a peculiar spectral shape, was reported by Brumm et al. (1992), Reinl et al. (1992), and Dolainsky et al. (1993), and the elliptical shape was shown clearly by electron microscopy of frozen MLV in the 9.4T magnetic field. The equation used for the simulations in Reinl et al. (1992) nevertheless is not correct and leads to exaggerated values of ellipticity. Therefore, we derived the equation that scales the intensity in the anisotropic spectrum according to an ellipsoidal distribution of bilayer normals with respect to the magnetic field (see Appendix). Assuming that the density of molecules is constant over the ellipsoidal surface, this probability function can be written as

$$P(\theta)\,d\theta = 2\pi c^2\left(\frac{\sin\theta}{[\sin^2\theta + (c/a)^2\cos^2\theta]^2}\right)d\theta,$$

where θ is the angle between the director axis (bilayer normal) and the magnetic field direction and c and a are the semimajor and semiminor ellipse axes, respectively. This equation thus was used to perform spectral simulations of the anisotropic ^{31}P-NMR spectra. It must be mentioned that all of the anisotropic signal was taken as coming from vesicles that depart from spherical shape under the action of the magnetic field. Experimental and simulated ^{31}P-NMR spectra (*solid* and *dashed* lines, respectively) are shown in Fig. 7. Besides spectra, the corresponding ellipsoids of the DPPC/cholesterol/melittin system ($R_i = 20$) are represented. The maximum of magnetically induced deformation is reached at 45° with a ratio of long/short ellipsoidal axis of 2. This temperature corresponds also to the maximum of membrane fragmentation (see Fig. 2). The correlation between the extent of membrane disruption and magnetic orientation was obtained for most of the investigated samples. This is also true for $R_i = 10$. In contrast to the ^{31}P-NMR experiments, orientational behavior of the model membrane was not observed in the case of ^{2}H-NMR. This is may be related to the fact that the magnetic field used for these experiments is of lower strength (4.7T vs. 6.35T) and/or that the samples were not prepared in the same way, i.e., for the experiments with labeled cholesterol samples contained 200 mg of DPPC, whereas the ^{31}P-NMR experiments were carried out on sample of 50 mg of DPPC, the buffer volume being 1 ml in both cases. Because the extent of magnetically induced vesicles deformation is known to be very sensitive to sample preparation and viscosity of the medium (Qiu et al., 1993), high viscosity of membrane preparations may be expected to interfere with magnetically induced bilayer orientation (Jansson et al., 1990; Qiu et al., 1993).

The extent of deformation is apparently dependent on the toxin efficiency. Consequently, it appears to be obvious that although a large part of the membrane is transformed into small objects, not all of the peptide participates in these complexes. A rather large number of melittin molecules have to stay with the large vesicles to induce such a deformation. Indeed, if one assumes that the melittin/lipid ratio for the discs does not change upon cholesterol incorporation and that the sterol causes no strong changes in the partition coefficient of melittin ($(2.1 \pm 0.2) \cdot 10^3\ M^{-1}$ in POPC (Kuchinka and

Seelig, 1989)), only half of the melittin amount would be associated with the discoidal objects.

In the following, we will try to account for vesicle deformation on the basis of two physical mechanisms: (i) variation of membrane magnetic susceptibility or (ii) modification of membrane elastic properties upon melittin addition. There is a possibility for a change of the diamagnetic susceptibility, $\Delta\chi$, of the bilayer, due to the presence of the peptide, because amphiphatic α-helical peptides exhibit relatively large positive $\Delta\chi$ values of which the principal component lies along the helical axis (Worcester, 1978). If these peptides are bound to the bilayer, such that the helical axis were perpendicular to the bilayers plane, a parallel orientation of the membrane would be induced, i.e., an accentuated 0° position in the NMR powder patterns. This seems to be the case for biological membranes (Neugebauer et al., 1977), where apparently the $\Delta\chi$ of the helices overrides the influence of the lipids, which orient preferentially with the lipid molecular axis perpendicular to the external magnetic field (Hong et al., 1971; Seelig et al., 1985). This behavior also has been found for the case of gramicidin (Van Echteld et al., 1982). Obviously, the contrary is observed in our study. Unfortunately, there exist to our knowledge no data for the anisotropic diamagnetic susceptibility of melittin, so that no decision can be made whether $\Delta\chi$ of the toxin is not important enough to dominate that of the bilayer or whether the peptide is associated with the membrane parallel with respect to the bilayer plane. Albeit the orientation of melittin in these remaining vesicles is not yet determined, many studies propose a wedge form of the peptide within the membrane, i.e., a quasi-parallel to the bilayers plane (e.g., Frey and Tamm (1991) in the case of a wet bilayer), which would not interfere with the $\Delta\chi$ of the lipids or could even be cooperative. The latter implies a nonrandom distribution of the helices on the bilayers surface triggered by the external magnetic field. On the other hand, one may as well assume that the direct influence of melittin (via $\Delta\chi$) is negligible considering the lipid/peptide molar ratio.

Membrane elastic properties may be modified (ii) by creation of defect structures in the membrane upon addition of melittin. Taking up the cluster model, as described above, it seems easily understandable that defects, or defect lines, will make the membrane in a macroscopic way more flexible. As it has been proposed, melittin would enter deeply into the bilayer's core at the interfacial areas, and this could result in a destabilization of the membrane. Defect lines with high incorporation of the peptide should allow a greater flexibility of the membrane than found for the toxin-free system. This would facilitate the ellipsoidal deformation of a vesicle in a magnetic/electric field or by mechanical forces. This would imply the idea of preformed discs in the membrane as in a *patchwork*. A quasi-similar approach might be made by invoking the pore-forming character of melittin (Tosteson and Tosteson, 1984; Alder et al., 1991), where the underlying idea is a transbilayer and oligomeric orientation of the peptide in the membrane. Although we favor a dynamical *patchwork* model, both approaches appear to be quite similar.

Finally, we would like to emphasize that a significant extent of magnetically induced membrane deformation is already observed for weak amounts of melittin ($R_i = 100$). At this concentration, the fragmentation of the system is not largely reduced in comparison with the cholesterol-free system. One might question what consequence has the incorporation of 30 mol% cholesterol on the melittin-induced *lysis*. There is no doubt that cholesterol is able to inhibit the fragmentation caused by the peptide, but phenomena like melittin-triggered vesicle deformation in the magnetic field might give rise to some doubt about the capability of cholesterol to inhibit lysis. Further investigations are required to clear up that point and to give more insight into the unique role of cholesterol in biology.

CONCLUSION

Broad line, solid state NMR appears to be an appropriate means to probe both macroscopic and microscopic perturbations as promoted by melittin on cholesterol-containing DPPC membranes. By taking advantage of the chemical shielding and the electric quadrupolar interactions, it was possible to follow both the phospholipid and the deuterated cholesterol in melittin-phospholipid-cholesterol systems and determine the lipid composition of newly formed complexes. In our study, the above allowed us to understand disc stability by regulation of their cholesterol content. Calculation of order parameter from deuterium spectra permitted an estimation of the thickness of discs and put forward a model of assembly for lipids and melittin. Modification of phosphorus-31 powder pattern lineshape allowed us to quantitize vesicle deformation as promoted by melittin and the external magnetic field and to demonstrate a close link between disc appearance and vesicle deformation. Such approaches should be considered to be powerful means to follow structural and mechanical properties of membranes and monitor the effects of electric, magnetic, or mechanic constrains that may be exerted on such systems.

We are grateful to Dr. Marin Mitov (Bulgarian Academy of Sciences) for help in calculating the ellipsoidal distribution probability and to Dr. Jean Dufourcq for very stimulating discussions.

APPENDIX

Ellipsoidal distribution probability of membrane normals, $\vec{n}$

Let us consider a prolate vesicle whose long axis (semimajor axis, c) is aligned with the external magnetic field. For such a vesicle, the normal to the bilayer does not pass necessarily through the center of the ellipsoid (Fig. 8). As a consequence, the angle θ between $\vec{n}$ and the magnetic field has to be correlated to the angles β and φ, which define the position of a point on the ellipsoidal surface:

$$x = \rho \cos\varphi \sin\beta$$
$$y = \rho \sin\varphi \sin\beta \qquad \text{(A1)}$$
$$z = \rho \cos\beta.$$

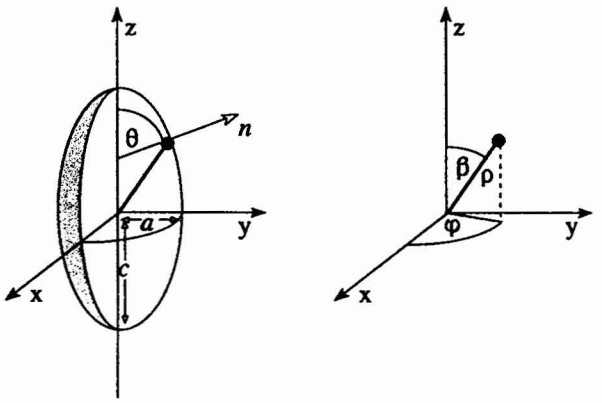

FIGURE 8 Definition of parameters for an ellipsoid with its long axis (c) aligned with the magnetic fiel direction. ρ, β, and φ: coordinates to define the position of a point on the ellipsoidal surface; θ: angle between $\vec{n}$ and the magnetic field.

Using the equation of an ellipsoid,

$$\frac{x^2 + y^2}{a^2} + \frac{z^2}{c^2} - 1 = 0, \tag{A2}$$

where a is the semiminor axis, Eq. A1 becomes

$$x = \frac{c}{\sqrt{D}} \cos\varphi \sin\beta$$

$$y = \frac{c}{\sqrt{D}} \sin\varphi \sin\beta \tag{A3}$$

$$z = \frac{c}{\sqrt{D}} \cos\beta,$$

with

$$D = 1 + e \sin^2\beta \qquad \text{and} \qquad e = \frac{c^2 - a^2}{a^2}.$$

The surface element of an ellipsoid can then be defined as

$$ds = c^2 \frac{\sqrt{\cos^2\beta + (1+e)^2 \sin^2\beta}}{D^2} \sin\beta \, d\beta \, d\varphi. \tag{A4}$$

The angle β must now be related to θ, the angle between $\vec{n}$ and B_0, i.e., the angle of interest. The normal to the surface is defined by

$$\vec{n} = \frac{\vec{n}_\beta \wedge \vec{n}_\varphi}{|\vec{n}_\beta \wedge \vec{n}_\varphi|}, \tag{A5}$$

where $\vec{n}_\beta$ and $\vec{n}_\varphi$ are the partial derivatives in β and φ:

$$\vec{n}_\beta = \frac{c}{D^{3/2}} \begin{bmatrix} \cos\beta\cos\varphi \\ \cos\beta\sin\varphi \\ -\sin\beta(1+e) \end{bmatrix} \qquad \vec{n}_\varphi = \frac{c}{D^{1/2}} \begin{bmatrix} -\sin\beta\sin\varphi \\ \sin\beta\cos\varphi \\ 0 \end{bmatrix}. \tag{A6}$$

The n_z coordinate is then given by

$$n_z = \frac{\cos\beta}{\sqrt{\cos^2\beta + (1+e)^2 \sin^2\beta}} \tag{A7}$$

and is also related to θ by $n_z = \cos\theta$, which leads to

$$\tan\theta = (1+e)\tan\beta. \tag{A8}$$

The probability density, $P(\theta)$, of having the normal, $\vec{n}$, of a surface element oriented at an angle θ with respect to the magnetic field is proportional to the area of a surface element. Making use of Eq. A8 and integrating Eq. A4 over φ leads to

$$P(\theta)\, d\theta = 2\pi c^2 \left(\frac{\sin\theta}{[\sin^2\theta + (c/a)^2 \cos^2\theta]^2} \right) d\theta. \tag{A9}$$

Equation A9 obviously reduces to $2\pi c^2 \sin\theta \, d\theta$ for the case of a sphere ($c = a$).

REFERENCES

Alder, G. M., W. M. Arnold, C. L. Bashford, A. F. Drake, C. A. Pasternak, and U. Zimmermann. 1991. Divalent cation-sensitive pores formed by natural and synthetic melittin and by triton X-100. *Biochim. Biophys. Acta.* 1061:111–120.

Batenburg, A. M., and B. De Kruijff. 1988. Modulation of membrane surface curvature by peptide-lipid interactions. *Biosci. Rep.* 8:299–307.

Bello, J., H. R. Bello, and E. Granados. 1982. Conformation and aggregation of melittin: dependence on pH and concentration. *Biochemistry.* 21: 461–465.

Bloom, M., J. H. Davis, and F. W. Dahlquist. 1978. Determination of Orientational Order in Bilayer Systems Using Moments of Deuterium Magnetic Resonance Spectra. E. Lipperan and T. Salveres, editors. 20th Ampere Congress. Springer-Verlag, Berlin. p. 551.

Bloom, M., J. H. Davis, and A. L. MacKay. 1981. Direct determination of the oriented sample NMR spectrum from the powder spectrum for systems with local axial symmetry. *Chem. Phys. Lett.* 80:198–202.

Brauner, J. W., R. Mendelsohn, and F. G. Prendergast. 1987. Attenuated total reflectance fourier transform infrared studies of the interaction of melittin, two fragments of melittin, and δ-hemolysin with phosphatidylcholines. *Biochemistry.* 26:8151–8158.

Brown, M. F., and J. Seelig. 1978. Influence of cholesterol on the polar region of phosphatidylcholine and phosphatidylethanolamine bilayers. *Biochemistry.* 17:381–384.

Brumm, T., A. Möps, C. Dolainsky, S. Brückner, and T. M. Bayerl. 1992. Macroscopic orientation effects in broadline NMR-spectra of model membranes at high magnetic field strength. A method preventing such effects. *Biophys. J.* 61:1018–1024.

Burnell, E. E., P. R. Cullis, and B. de Kruijff. 1980. Effects of tumbling and lateral diffusion on phosphatidylcholine model membrane ^{31}P-NMR lineshapes. *Biochim. Biophys. Acta.* 603:63–69.

Burnett, L. J., and B. H. Müller. 1978. Deuteron quadrupolar coupling constants in three solid deuterated paraffin hydrocarbons: C_2D_6, C_4D_{10}, C_6D_{14}. *J. Chem. Phys.* 55:5829–5831.

Cruzeiro-Hansson, L., J. H. Ipsen, and O. G. Mouritsen. 1989. Intrinsic molecules in lipid membranes change the lipid-domain interfacial area: cholesterol at domain interfaces. *Biochim. Biophys. Acta.* 979:166–176.

Dasseux, J. L., J. F. Faucon, M. Lafleur, M. Pezolet, and J. Dufourcq. 1984. A restatement of melittin-induced effects on the thermotropism of zwitterionic phospholipids. *Biochim. Biophys. Acta.* 755:37–50.

Davis, J. H. 1979. Deuterium magnetic resonance study of the gel and liquid crystalline phases of dipalmitoylphosphatidylcholine. *Biophys. J.* 27:339–358.

Dawson, C. R., A. F. Drake, J. Heliwell, and R. C. Hider. 1978. The interaction of melittin with lipid bilayers. *Biochim. Biophys. Acta.* 510:75*a*. (Abstr.)

Dempsey, C. E. 1990. The action of melittin on membranes. *Biochim. Biophys. Acta.* 1031:143–161.

Dempsey, C. E., and B. Sternberg. 1991. Reversible disc-micellization of DMPC bilayers induced by melittin and [Ala-14] melittin. *Biochim. Biophys. Acta.* 1061:175–184.

Dempsey, C. E., and A. Watts. 1987. A deuterium and phosphorus-31 NMR study of the interaction of melittin with dimyristoylphophatidylcholine bilayers and the effect of contaminating phospholipase A_2. *Biochemistry.* 26:5803–5811.

Dolainsky, C., A. Möps, and T. M. Bayerl. 1993. Transversal relaxation in supported and nonsupported phospholipid model membranes and the influence of ultraslow motions: a ^{31}P-NMR study. *J. Chem. Phys.* 98:1712–1720.

Douliez, J. P., A. M. Bellocq, and E. J. Dufourc. 1994. Effect of vesicle size, polydispersity and multilayering on solid state ^{31}P- and ^{2}H-NMR spectra. *J. Chem. Phys.* 91:874–880.

Drake, A. F., and R. C. Hider. 1979. The structure of melittin in lipid bilayer membranes. *Biochim. Biophys. Acta.* 555:371–373.

Dufourc, E. J., J. M. Bonmatin, and J. Dufourcq. 1989. Membrane structure and dynamics by ^{2}H and ^{31}P-NMR. Effects of amphipatic peptidic toxins on biological membranes. *Biochimie.* 71:117–123.

Dufourcq, J., and J. F. Faucon. 1977. Intrinsic fluorescence study of lipid-protein interactions in membrane models: binding of melittin, an amphiphatic peptide, to phospholipids vesicles. *Biochim. Biophys. Acta.* 467:1–11.

Dufourcq, J., J. F. Faucon, G. Fourche, J. L. Dasseux, M. Le Maire, and T. Gulik-Krzywicki. 1986. Morphological changes of phosphatidylcholine bilayers induced by melittin: vesicularization, fusion, discoidal particles. *Biochim. Biophys. Acta.* 859:33–48.

Dufourc, E. J., J. F. Faucon, G. Fourche, J. Dufourcq, T. Gulik-Krzywicki, and M. Le Maire. 1986a. Reversible disc-to-vesicle transition of melittin-DPPC complexes triggered by the phospholipid acyl chain melting. *FEBS Lett.* 201:205–209.

Dufourc, E. J., C. Mayer, J. Stohrer, and G. Kothe. 1992. ^{31}P and ^{1}H-NMR pulse sequences to measure lineshapes, T_{1Z} and T_{2E} relaxation times in biological membranes. *J. Chem. Phys.* 89:243–252.

Dufourc, E. J., E. J. Parish, S. Chitrakorn, and I. C. P. Smith. 1984. Structural and dynamical details of cholesterol-lipid interactions as revealed by ^{2}H-NMR. *Biochemistry.* 23:6062–6071.

Dufourc, E. J., I. C. P. Smith, and J. Dufourcq. 1986b. Molecular details of melittin-induced lysis of phospholipid membranes as revealed by deuterium and phosphorus NMR. *Biochemistry.* 25:6448–6455.

Faucon, J. F., J. Dufourcq, and C. Lussan. 1979. The self-association of melittin and its binding to lipids—an intrinsic fluorescence polarization study. *FEBS Lett.* 102:187–190.

Frey, S., and L. K. Tamm. 1991. Orientation of melittin in phospholipid bilayers. *Biophys. J.* 60:922*a*. (Abstr.)

Habermann, E. 1972. Bee and wasp venoms. *Science.* 177:314–322.

Habermann, E., and J. Jentsch. 1967. Sequenzanalyse des Melittins aus seinen tryptischen und peptischen Spaltstücken. *Hoppe-Seyler's Z. Physiol. Chem.* 348:37–50.

Hong, F. F., D. Mauzerall, and A. Mauro. 1971. Magnetic anisotropy and the orientation of retinal rods in a homogeneous magnetic field. *Proc. Natl. Acad. Sci. USA.* 68:1283–1285.

Ipsen, J. H., G. Karlström, O. G. Mouritsen, H. Wennerström, and M. J. Zuckermann. 1987. Phase equilibria in the phosphatidylcholine-cholesterol system. *Biochim. Biophys. Acta.* 905:162–172.

Ipsen, J. H., O. G. Mouritsen, and M. J. Zuckermann. 1990. Theory of thermal anomalies in the specific heat of lipid bilayers containing cholesterol. *Biophys. J.* 56:661–667.

Jansson, M., R. L. Thurmond, T. P. Trouard, and M. F. Brown. 1990. Magnetic alignment and orientational order of dipalmitoylphosphatidylcholine bilayers containing palmitoyllysophosphatidylcholine. *Chem. Phys. Lipids.* 54:157–170.

John, E., and F. Jähnig. 1991. Aggregation state of melittin in lipid vesicles membranes. *Biophys. J.* 60:319*a*. (Abstr.)

Kuchinka, E., and J. Seelig. 1989. Interaction of melittin with phosphatidylcholine membranes. Binding isotherm and lipid head-group conformation. *Biochemistry.* 28:4216–4221.

Lauterwein, J., C. Bösch, L. R. Brown, and K. Wüthrich. 1979. Physicochemical studies of the protein-lipid interactions in melittin containing micelles. *Biochim. Biophys. Acta.* 556:244–264.

Léonard, A., and E. J. Dufourc. 1991. Interactions of cholesterol with the membrane lipid matrix. A solid state NMR approach. *Biochimie.* 73: 1295–1302.

Levitt, M. H. 1982. Symmetrical composite pulse sequence for NMR population inversion. I. Compensation of Radiofrequency field inhomogenity. *J. Magn. Reson.* 48:234–264.

Levitt, M. H., and R. Freeman. 1981. Compensation for pulse imperfections in NMR spin-echo experiments. *J. Magn. Reson.* 43:65–80.

MacDonald, J. C. 1980. Least-square fit to some NMR functions. *J. Magn. Reson.* 38:381–384.

Marbrey, S., P. L. Mateo, and J. M. Sturtevant. 1978. High-sensitivity differential scanning calorimetric study of mixtures of cholesterol with dimyristoyl- and dipalmitoylphosphatidylcholines. *Biochemistry.* 17:2464–2468.

Marcelja, S. 1974. Chain ordering in liquid crystals. II. Structure of bilayer membranes. *Biochim. Biophys. Acta.* 367:165–176.

Marsh, D. 1990. CRC Handbook of Lipid Bilayers. CRC Press, Boca Raton, FL. 386 pp.

Maurer, T., C. Lücke, and H. Rüterjans. 1991. Investigation of the membrane-active peptide melittin and glucagon by photochemically induced dynamic-nuclear-polarization (photo-CIDNP) NMR. *Eur. J. Biochem.* 196:135–141.

McMullen, T. P. W., R. N. A. H. Lewis, and R. N. McElhaney. 1993. Differential scanning calorimetrie of the effect of cholesterol on the thermotropic phase behavior of a homologous series of linear satured phosphatidylcholines. *Biochemistry.* 32:516–522.

Monette, M., M. R. van Calsteren, and M. Lafleur. 1993. Effect of cholesterol on the polymorphism of dipalmitoylphosphatidylcholine/melittin complexes: an NMR study. *Biochim. Biophys. Acta.* 1149:319–328.

Morrow, M. R., and D. Lu. 1991. Universal behavior of lipid acyl chain order: chain length scaling. *Chem. Phys. Lett.* 128:435–439.

Mouritsen, O. G., and M. Bloom. 1984. Mattress model of protein-lipid interactions in membranes. *Biophys. J.* 46:141–153.

Needham, O., T. J. McIntosh, and E. Evans. 1988. Thermodynamical transition properties of DMPC/cholesterol bilayers. *Biochemistry.* 27: 4668–4673.

Neugebauer, D. C., A. E. Blaurock, and D. L. Worcester. 1977. Magnetic orientation of purple membranes demonstrated by optical measurements and neutron scattering. *FEBS Lett.* 78:31–35.

Parasassi, T., M. Di Stefano, M. Loiero, G. Ravagnan, and E. Gratton. 1994. Influence of cholesterol on phospholipid bilayers phase domains as detected by laurdan fluorescence. *Biophys. J.* 66:120–132.

Podo, F., R. Strom, C. Crifo, and M. Zulauf. 1982. Dependence of melittin structure on its interaction with multivalent ions and lipid membranes. *Int. J. Peptide Protein Res.* 19:514–527.

Pott, T., and E. J. Dufourc. 1993. Cholesterol inhibits melittin-induced membrane lysis. A solid state 31P-NMR study. *Bull. Magn. Reson.* 15:121–123.

Qiu, X., P. A. Mirau, and C. Pidgeon. 1993. Magnetically induced orientation of phosphatidylcholine membranes. *Biochim. Biophys. Acta.* 1147:59–72.

Rance, M., and R. A. Byrd. 1983. Obtaining high-fidelity spin 1/2 powder spectra in anisotropic media: phase-cycled Hahn echo spectroscopy. *J. Magn. Reson.* 52:221–240.

Reinl, H., T. Brumm, and T. M. Bayerl. 1992. Changes of the physical properties of the liquid-ordered phase with temperature in binary mixtures of DPPC with cholesterol. *Biophys. J.* 61:1025–1035.

Sankaram, M. B., and T. E. Thompson. 1990. Interaction of cholesterol with various glycerophospholipids and sphingomyelin. *Biochemistry.* 29:10670–10675.

Schindler, H., and J. Seelig. 1975. Deuterium order parameters in relation to thermodynamic properties of a phospholipid bilayer. A statistical mechanical interpretation. *Biochemistry.* 14:2283–2287.

Scott, H. L. 1991. Lipid-cholesterol interactions. Monte Carlo simulations and theory. *Biophys. J.* 59:445–455.

Seelig, A., and J. Seelig. 1974. The dynamic structure of fatty acyl chains in a phosphatidylcholine bilayer measured by deuterium magnetic resonance. *Biochemistry.* 13:4839–4845.

Seelig, J., F. Borle, and T. A. Cross. 1985. Magnetic ordering of phospholipid membranes. *Biochim. Biophys. Acta.* 814:195–198.

Seelig, J., and A. Seelig. 1980. Lipid conformation in model membranes and biological membranes. *Q. Rev. Biophys.* 13:19–61.

Segrest, J. P. 1977. Amphipathic helixes and plasma lipoproteins: thermodynamic and geometric considerations. *Chem. Phys. Lipids.* 18:7–22.

Sessa, G., J. H. Freer, G. Colacicco, and G. Weismann. 1969. Interaction of a lytic polypeptide melittin with lipid membrane systems. *J. Biol. Chem.* 244:3575–3582.

Sternin, E., M. Bloom, and A. L. MacKay. 1983. De-Pake-ing of NMR Spectra. *J. Magn. Reson.* 55:274–282.

Talbot, J. C., J. Dufourcq, J. De Bony, J. F. Faucon, and C. Lussan. 1979. Conformational change and self-association of monomeric melittin. *FEBS Lett.* 102:191–193.

Talbot, J. C., J. F. Faucon, and J. Dufourcq. 1987. Different states of self-association of melittin in phospholipid bilayers. *Eur. Biophys. J.* 15:147*a*. (Abstr.)

Taylor, M. G., T. Akiyama, and I. C. P. Smith. 1981. The molecular dynamics of cholesterol in bilayer membranes: a deuterium NMR study. *Chem. Phys. Lipids.* 29:327–339.

Terwilliger, T. C., and D. Eisenberg. 1982. The structure of melittin I and II. *J. Biol. Chem.* 257:6010–6022.

Tosteson, M. T., and D. C. Tosteson. 1984. Activation and inactivation of melittin channels. *Biophys. J.* 45:112–114.

Van Echteld, C. J. A., B. De Kruijff, A. J. Verkleij, J. Leunissen-Bijvelt, and J. De Gier. 1982. Gramicidin induces the formation of non-bilayer structures in phosphatidylcholine dispersions in a fatty acid chain length dependent way. *Biochim. Biophys. Acta.* 692:126–138.

Vist, M. R., and J. H. Davis. 1990. Phase equilibria of cholesterol dipalmitoylphosphatidylcholine mixtures: ^{2}H-nuclear magnetic resonance and differential scanning calorimetry. *Biochemistry.* 29:451–464.

Vogel, H. 1987. Comparison of the conformation and orientation of alamethicin and melittin in lipid membranes. *Biochemistry.* 26:4562–4572.

Weaver, A. J., M. D. Kemple, J. W. Brauner, R. Mendelsohn, and F. G. Prendergast. 1992. Fluorescence, CD, Attenuated total reflectance (ATR) FTIR and ^{13}C NMR characterization of the structure and dynamics of synthetic melittin and melittin analogues in lipid environments. *Biochemistry.* 31:1301–1313.

Worcester, D. L. 1978. Structural origins of diamagnetic susceptibility in proteins. *Proc. Natl. Acad. Sci. USA.* 75:5475–5477.

Yeagle, P. L. 1985. Cholesterol and the cell membrane. *Biochim. Biophys. Acta.* 822:267–287.